Layer Outcropping in Numerical Models of Stratified Flows

SHAN SUN,* RAINER BLECK, AND ERIC P. CHASSIGNET

Rosenstiel School of Marine and Atmospheric Science, University of Miami, Miami, Florida

23 March 1992 and 17 November 1992

ABSTRACT

Layered models of stratified flow are favored by theoreticians because of their conceptual simplicity but have only seen limited use in numerical modeling due to difficulties related to layer outcropping (vanishing layer depth). Two mass transport schemes capable of handling outcropping are tested against analytic solutions describing wind- and buoyancy-forced flow in a two- and three-layer ocean. In both cases, the model is found to closely reproduce the available analytic solutions. This result helps alleviate longstanding reservations about the severity of the outcrop problem in layer models.

1. Introduction

The practical use of a buoyancy-related variable—potential density in water or potential temperature in air—as vertical coordinate in describing motion in stratified geophysical fluids dates back to Rossby et al. (1937) and Montgomery (1937). The dynamic equations resulting from this change in vertical coordinate have formed the basis of numerous theoretical investigations. Geometric height, on the other hand, became the vertical coordinate of choice in early numerical ocean models. As a result, a significant gap has developed in the past two decades between numerical and analytic models. To close this gap, the real and perceived obstacles that have impeded model design along the lines favored by theoreticians should be reconsidered.

Perhaps the most elegant way to construct a three-dimensional density-coordinate numerical model (the word "density" stands here for any variable expressing the buoyancy of a fluid parcel) is to form a stack of two-dimensional shallow water models, arranged such that lighter fluid layers rest on top of denser layers. The resulting discrete-layer structure is a valid finite-difference approximation to the continuous equations transformed to density coordinates, giving rise, of course, to vertical truncation errors, which can be suppressed by increasing the number of layers. The fact that a density-coordinate *layer* model has an exact physical analog (at least as far as vertical discretization is concerned) makes this a very attractive concept in model building.

One of the numerical difficulties associated with such layer models is readily apparent. Since horizontal density gradients along the top or bottom of the fluid play an essential role in baroclinic instability and thus in the oceanic and atmospheric general circulation, density-coordinate layer models will be of limited utility as long as they do not permit coordinate layers to "outcrop," that is, intersect the upper or lower boundary. To be fully general, outcrop locations furthermore must be allowed to vary with time. Mathematically, this is equivalent to allowing individual layers to vanish or "dry up" wherever and whenever this is called for by the underlying dynamic processes. In other words, the algorithm for solving the shallow water continuity equation in a layer model must be equipped to handle the transition in time and space between zero and nonzero layer thickness. This turns out to be a nontrivial matter.

The problem just described has been sidestepped in many previous ocean modeling studies by choosing a sufficiently thick upper layer (Holland and Lin 1975; Hurlburt and Thompson 1980; Luther and O'Brien 1985; Woodberry et al. 1989; Thompson and Schmitz 1989) or by the use of hybrid coordinates (Bleck and Boudra 1981). Only in the last decade have geophysical fluid modelers acquired the know-how to model ocean circulation regimes that include outcropping layers. Today we have a number of algorithms at our disposal that maintain positive-definiteness in the layer-thickness field without being excessively diffusive, that is, without sacrificing numerical accuracy to a great extent. Early papers dealing successfully with the outcropping issue include those of Bogue et al. (1986), Bleck and Boudra (1986), and Huang (1986, 1987). They all used the flux-corrected transport (FCT) algorithm (Boris and Book 1973; Zalesak 1979) to solve the shallow water continuity equation.

Even today, outcropping remains the Achilles heel of density-coordinate layer models. It therefore seems

* Current affiliation: NOAA/ERL/Forecast Systems Laboratory, Boulder, Colorado.

Corresponding author address: Dr. Rainer Bleck, RSMAS, Division of Meteorology and Physical Oceanography, University of Miami, 4600 Rickenbacker Causeway, Miami, FL 33149-1098.

prudent to continue, as Bogue et al. (1986) did, to search for nontrivial analytic solutions of circulation problems that can be used to test the numerical model's accuracy. With more than one positive-definite transport scheme at our disposal today, such experiments can be made even more rewarding by including an intercomparison of several numerical algorithms.

In this note, the capabilities of two numerical schemes designed to handle zero layer thickness in shallow water models are discussed by comparing model-generated simulations to analytic solutions. The two algorithms considered are the aforementioned FCT algorithm and the multidimensional positive-definite advection transport algorithm (MPDATA) scheme (Smolarkiewicz 1984; Smolarkiewicz and Clark 1986; Smolarkiewicz and Grabowski 1990). We use as a framework the isopycnic-coordinate primitive equation model of Bleck and Boudra (1986) configured on a β plane in a rectangular, flat-bottom ocean basin and forced by either wind stress or buoyancy fluxes.

2. The numerical schemes

The shallow-water continuity equation, which is solved in each coordinate layer together with the horizontal momentum equations, may be written as

$$\frac{\partial h}{\partial t} + \nabla\cdot(h\mathbf{v}) = 0, \tag{1}$$

where h is the layer thickness and $\mathbf{v} = (u, v)$ is the horizontal velocity vector. [For a discussion of the precise meaning of the word "horizontal," see Bleck (1978).] If one replaces $h\mathbf{v}$ in (1) by a conventional second- or higher-order finite-difference expression ("order" refers here to the power of the mesh size in the leading term of the truncation error), h can change sign during integration of (1) over a finite time step Δt if $\nabla\cdot(h\mathbf{v})$ is large and h is already near zero at the beginning of Δt. This is, of course, most likely to happen in the outcropping region.

The use in (1) of the diffusive, first-order forward-upstream scheme

$$h_{ij}^{n+1} = h_{ij}^{n} - \Delta t\left(\frac{U_{i+1/2,j}^{n} - U_{i-1/2,j}^{n}}{\Delta x} + \frac{V_{i,j+1/2}^{n} - V_{i,j-1/2}^{n}}{\Delta y}\right), \tag{2}$$

with

$$U_{i-1/2,j}^{n} = \begin{cases} u_{i-1/2,j}^{n} h_{i-1,j}^{n} & \text{if} \quad u_{i-1/2,j}^{n} > 0 \\ u_{i-1/2,j}^{n} h_{i,j}^{n} & \text{if} \quad u_{i-1/2,j}^{n} < 0, \end{cases} \tag{3}$$

(the other three flux expressions formulated analogously) is known to keep h positive definite. Thus, the primary reason for using more elaborate schemes like FCT and MPDATA is to reduce numerical diffusion. In fact, both schemes mentioned advance the h field over Δt by first doing a forward-upstream transport step, followed by an elaborate "antidiffusive" correction step. Computing the antidiffusive fluxes used in the second step is itself a two-step process. First, provisional antidiffusive fluxes are defined which, if used unaltered, would remove from the h field the essential part of the low-order truncation error introduced by (2). The provisional fluxes are subsequently altered to some extent to prevent them from introducing additional ripples, including sign changes, in the h field.

In the FCT scheme, the provisional antidiffusive fluxes are given by the difference between high-order and low-order finite-difference expressions for $h\mathbf{v}$:

$$(h\mathbf{v})^{\text{anti}} = (h\mathbf{v})^{\text{high}} - (h\mathbf{v})^{\text{low}}. \tag{4}$$

In the present study, second-order, space-centered expressions of the form

$$U_{i-1/2,j}^{n} = u_{i-1/2,j}^{n}\frac{h_{i-1,j}^{n} + h_{i,j}^{n}}{2}$$

serve as high-order fluxes, while the low-order fluxes are those given in (3). Note that the FCT algorithm leaves aside the temporal part of the truncation error of the low-order scheme.

In the MPDATA scheme, provisional antidiffusive velocities and fluxes are given by the leading term of the temporal/spatial truncation error of (2). Removal of this part of the truncation error elevates the scheme as a whole to third-order accuracy in space and time, in contrast to the FCT scheme where the user is able to specify the desired spatial (but only the spatial) order of the high-order transport process.

Specifically, the provisional antidiffusive fluxes in the MPDATA scheme are given by

$$(hu)^{\text{anti}} = \frac{1}{2}(|u|\Delta x - u^2\Delta t)\frac{\partial h}{\partial x} - \frac{uv\Delta t}{2}\frac{\partial h}{\partial y},$$

$$(hv)^{\text{anti}} = \frac{1}{2}(|v|\Delta y - v^2\Delta t)\frac{\partial h}{\partial y} - \frac{uv\Delta t}{2}\frac{\partial h}{\partial x}.$$

The extent to which the above antidiffusive fluxes must be reduced to prevent over- and undershooting is determined as follows. Consider the four antidiffusive fluxes that flow through the four sides of a given grid box. Let $\mu_{\text{in}} \leq 1$ be the factor by which the *inward*-directed fluxes acting in concert would have to be multiplied to prevent h in the box from exceeding a given upper bound. (The effect of outgoing fluxes, if any, is disregarded in calculating μ_{in}.) Likewise, let $\mu_{\text{out}} \leq 1$ be the factor by which the *outgoing* fluxes would have to be multiplied to prevent h from falling below a prescribed lower bound. The upper and lower bounds are usually set to the largest and smallest of the four surrounding h values, respectively, resulting from the preceding forward-upstream transport step.

Consider now an individual antidiffusive flux directed from, say, grid box 1 to grid box 2. This flux is subject to two requirements—no undershooting allowed in box 1 and no overshooting allowed in box 2.

Both requirements can be satisfied if the given flux value is multiplied by a factor μ, which is the lesser of μ_{out} for box 1 and μ_{in} for box 2.

An additional step is required in numerical models that use a modified rigid-lid approximation (a time-invariant bottom pressure condition, to be precise) to filter out barotropic gravity waves, such as the one of Bleck and Boudra (1986). Suppose the high-order fluxes used in the FCT scheme are formulated so as to yield zero barotropic mass flux divergence, that is, maintain bottom pressure. Clipping of antidiffusive fluxes (multiplication by μ) will then lead to bottom pressure changes in grid boxes affected by the clipped fluxes. To force the total mass flux field to preserve bottom pressure, the fluxes $(1 - \mu)(h\mathbf{v})^{anti}$ discarded in the clipping process must be accounted for. This is done, as described by Bleck and Boudra (1986), by vertically summing up the discarded flux portions and adding them as barotropic corrections to the antidiffusive mass fluxes. By prorating the corrective flux among individual layers according to the h distribution in the *upstream* column, this final modification of the mass field will not violate the requirement $h \geq 0$.

As outlined earlier, antidiffusive fluxes in the original MPDATA scheme are not formulated on the basis of a specific high-order flux expression. However, high-order fluxes that by design conserve bottom pressure do come into play in the MPDATA scheme as bottom pressure is being restored. The particulars of this process are as follows. As in the FCT case, fluxes that represent the difference between the actual and the bottom pressure–preserving high-order fluxes are being summed up vertically. In the MPDATA case these fluxes have the form

$$(h\mathbf{v})^{high} - \mu(h\mathbf{v})^{anti},$$

where, as before, $\mu = \min(\mu_{in}, \mu_{out})$. Prorating the fluxes among individual coordinate layers is done as described above.

3. The numerical experiments

a. *Huang's solution*

Huang (1984, 1986) and Huang and Flierl (1987) show that essential aspects of the circulation in a two-layer, two-gyre wind-forced ocean basin (one aspect being the size of the outcrop region) are controlled by a single nondimensional number $\lambda = \tau_m L/g'H_1^2$, where τ_m is the maximum wind stress; L the basin width; $g' = g\Delta\rho/\rho$ the buoyancy difference between the two layers; and H_1 the mean upper-layer thickness. The nonlinearity associated with layer depth changes is included in these studies, but the inertial terms in the momentum equations are omitted.

One of Huang's (1984) analytic solutions for a finite-depth lower layer (Fig. 1a,b) has been reproduced numerically. The analytic development of Huang (1984) requires a small ratio $\delta = H_1/H_2$; the two-layer numerical experiment therefore possesses a relatively thin upper layer (H_1 = 150 m) and thick lower layer (H_2 = 4850 m), which correspond to $\delta = 1/30$. The other parameters τ_m, L, and g' were chosen such that λ = 0.30 yields an outcrop region that spans virtually the entire cyclonically forced region and extends into the anticyclonically forced region (Fig. 1a,b). Dissipation is achieved by a vertical diffusion term with a constant eddy viscosity A whose strength is characterized by the dimensionless number $\epsilon = (2A/f)^{1/2}/H_1$ [see Huang (1984) for more details]. The analytic solution in Fig. 1a,b was obtained with ϵ = 0.03.

After approximately five years of integration, the model reaches a steady state characterized by upper- and lower-layer mass transport streamfunctions shown in Fig. 1. Model results based on FCT are displayed in Fig. 1c,d; model results based on MPDATA in Fig. 1e, f. As in the analytic solution (Fig. 1a,b), the outcrop area in both figures is observed to extend south of the latitude of maximum wind stress (the zero wind stress curl line, ZWCL). The upper- and lower-layer flow combine to reduce the total mass flux across the ZWCL to zero, satisfying the Sverdrup balance.

The two numerical solutions are in fair agreement with the analytic results of Fig. 1a,b. The major difference is found in the southwest corner of the outcrop area where the layer thickness gradient is weaker in the two numerical solutions. Total agreement between numerical and analytic solutions cannot be expected here since the analytic solution is obtained by patching up solutions obtained independently for the basin interior and the boundary current region (Huang 1984). The boundary-layer width associated with ϵ = 0.03 is quite large (75 km) and is double that value at the point where the western boundary current separates. This aspect is not taken into account in the analytic solution. As shown in Fig. 1g,h and Fig. 1i, j, a reduction of ϵ by a factor 3 and 6, respectively, leads to a narrower jet and the elimination of the weak layer thickness gradient in Fig. 1c,d. A similar result is obtained when the dissipation term is formulated with a horizontal eddy viscosity (Chassignet and Bleck 1993) (Fig. 1k,l).

Two differences between the two numerical solutions are apparent: 1) the outcrop area in the MPDATA case (Fig. 1e) is slightly smaller than in the FCT case (Fig. 1c) and 2) the front associated with the outcrop is narrower in the FCT solution. This translates into a stronger layer-thickness gradient and consequently stronger flows. Overall, the MPDATA solution appears to be slightly more diffusive, resulting in a smaller outcrop area, a broader frontal zone, and a weaker circulation. The FCT solution appears to be more able to reproduce steep gradients at the outcropping line.

b. *Dewar's solution*

Dewar (1991) obtained analytic solutions describing steady-state, buoyancy-driven flow in the interior of a

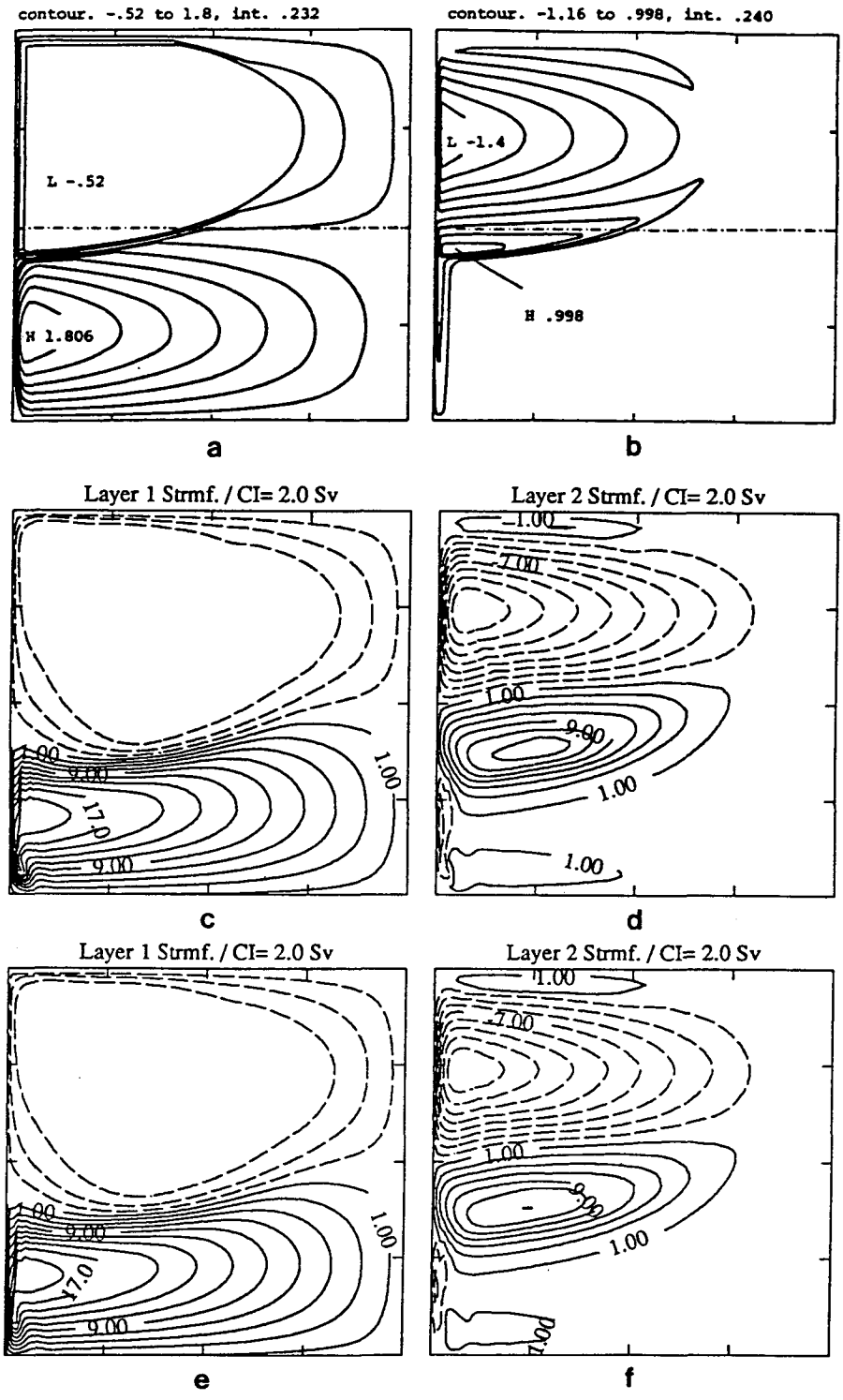

FIG. 1. Mass transport streamfunction in upper layer (left) and lower layer (right) for (a) and (b) analytic solution, $\epsilon = 0.03$ (Huang 1984; nondimensional units correspond to $\sim 12 \times 10^6$ $m^3 s^{-1}$); (c) and (d) FCT solution, $\epsilon = 0.03$; (e) and (f) MPDATA solution, $\epsilon = 0.03$; (g) and

three-layer ocean bounded to the east. His necessarily simplified parameterization of buoyancy-induced interfacial mass fluxes leads to surfacing of the second layer (outcropping) in the cooled part of the basin and "pinches off" of the second layer (incropping) in the heated part of the basin.

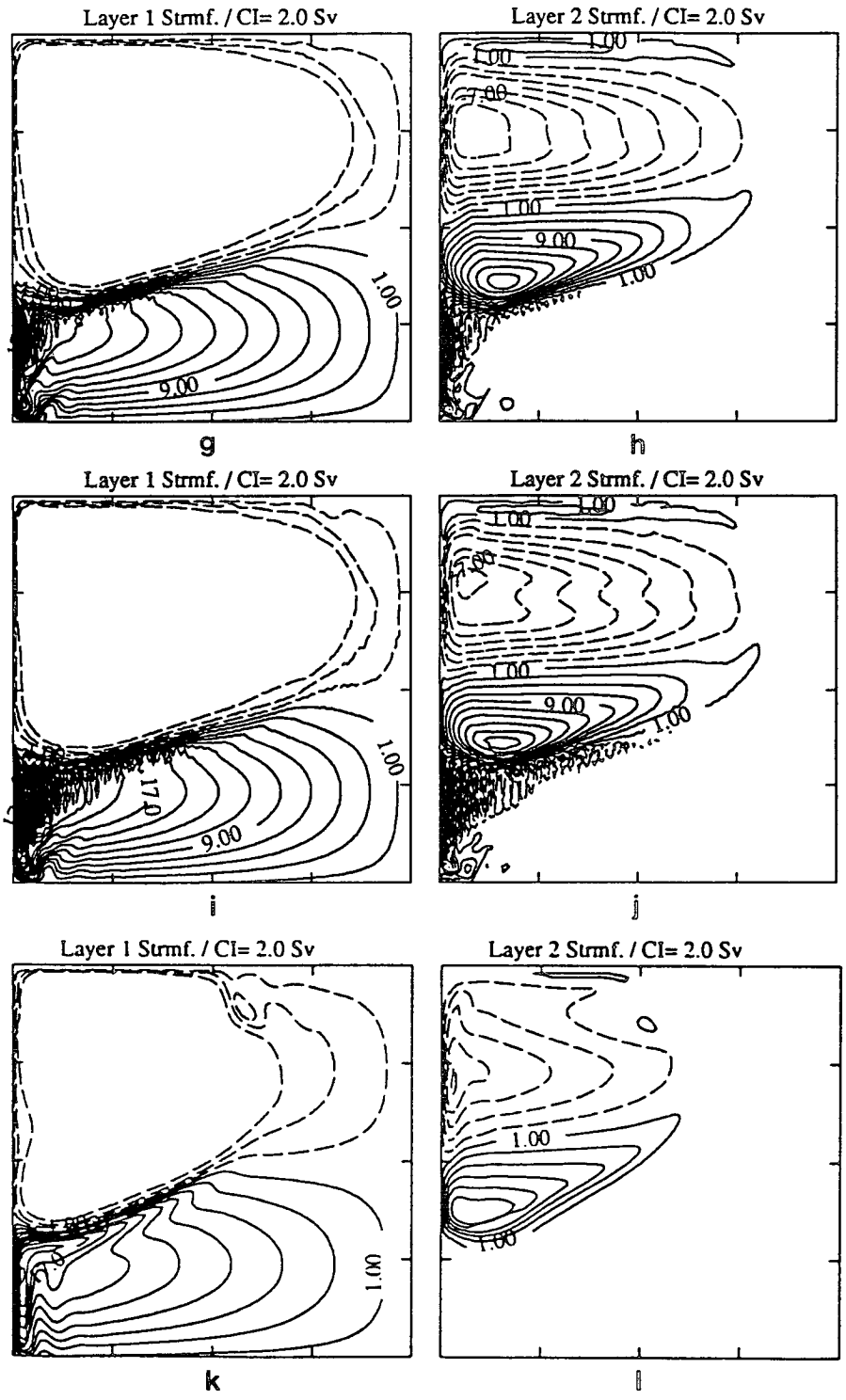

FIG. 1. (*Continued*) (h) FCT solution, $\epsilon = 0.01$; (i) and (j) FCT solution, $\epsilon = 0.005$; and (k) and (l) FCT solution, horizontal eddy viscosity 200 $m^2\ s^{-1}$.

As stated, Dewar's analytic solutions are valid in an open ocean basin bounded only on one side, while our numerical model describes flow in a closed basin. A meaningful comparison between the analytic and the numerical solution can therefore be made only in the basin interior. By choosing a realistic amplitude for the buoyancy forcing function, Dewar (1991) is able to obtain a physically meaningful solution in a square

domain measuring 5000 km on the side. We have added to this a buffer zone 1250-km wide to the north, south, and west to accommodate the return flow, thereby arriving at a rectangular basin measuring 7500 km in meridional and 6250 km in zonal direction.

Figures 2a,b,c,d show the top layer thickness of the analytic solution and of the numerical solution obtained with the FCT, MPDATA, and the forward-upstream scheme, respectively. It appears that the flow in the northern part of the basin is less zonal in the MPDATA solution than in the FCT solution and as such is closer to the analytic solution. The pressure gradient near the outcropping region is weaker in the MPDATA solution than in the FCT solution, suggesting that the former is more diffusive than the latter.

As seen in Fig. 2d, the forward-upstream solution (zero antidiffusive fluxes) does not show upper-layer outcropping. Thus, the low-order scheme does not correctly represent the character of the buoyancy-driven circulation, further evidence for the need to include an antidiffusive step.

Vertical sections indicating the layer structure are shown in Fig. 2. The extent of both the outcropping and the incropping area in the analytic solution is matched more closely by the MPDATA than the FCT solution. The average slope of the first interface, as measured by the distance between the outcropping and incropping zone, is larger in the FCT case.

In Dewar's (1991) solution, the bottom layer is motionless except in regions where the three layers are reduced to two. Thus, the velocity field in the third layer is discontinuous across the perimeter of both the first-layer outcropping zone and the second-layer incropping zone. Since the model momentum equations include a viscous term while the analytic solution does not, this discontinuity and the accompanying sharp reversal of lower interface slope (see Fig. 3a) is not captured in the numerical model.

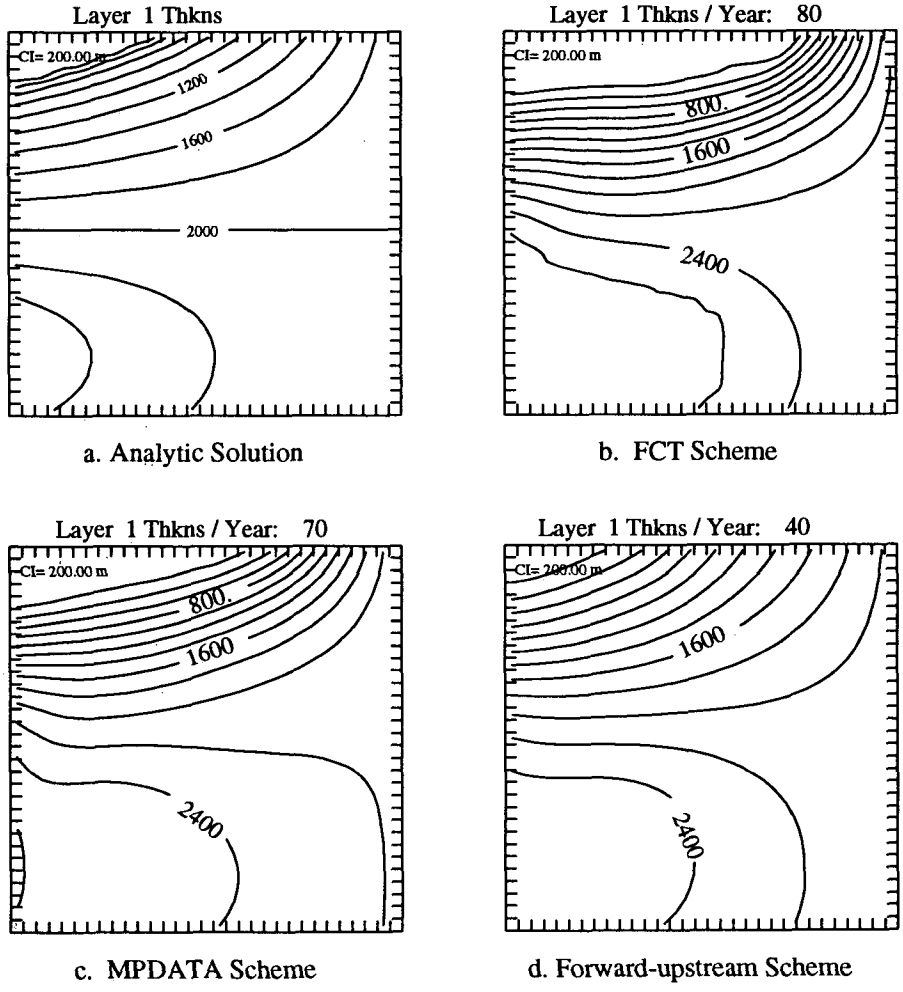

FIG. 2. Upper-layer thickness (m). (a) Analytic solution (Dewar 1991), (b) FCT solution, (c) MPDATA solution, and (d) forward-upstream solution.

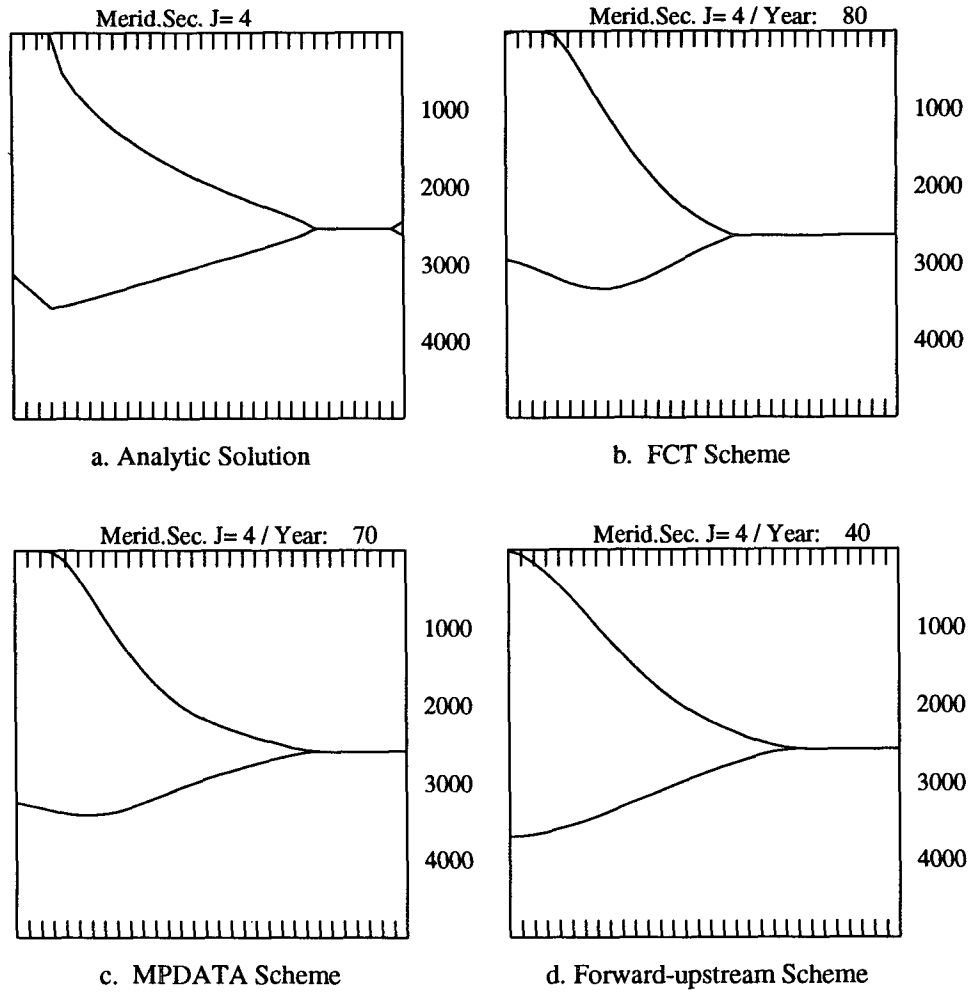

FIG. 3. Interface depth (m) vs latitude (N at left) for (a) analytic solution (Dewar 1991), (b) FCT solution, (c) MPDATA solution, and (d) forward-upstream solution.

Judging from a time trace of kinetic energy, the model using the forward-upstream scheme reaches an approximate steady state after roughly 45 years, whereas the models employing MPDATA and FCT take 65 and 75 years, respectively. The fact that the FCT-based solution takes longest to come to an equilibrium is consistent with the previously expressed notion that the FCT scheme is the least diffusive of the three schemes.

4. Summary and concluding remarks

The credibility and general utility of primitive equation layer models depends to some extent on their ability to reproduce isopycnic layer outcropping at the surface or the ocean bottom. Our goal in this note has been to shed light on the question of how closely numerical transport schemes come to reproducing analytic solutions describing stratified flow on a β plane that include layer outcropping. An ancillary question is whether a time-dependent, externally forced model would approach the state described by the analytic solutions, or whether it would converge toward some other final state. Our contribution may be viewed as an extension of the work by Bogue et al. (1986) to analytic solutions found only in recent years. We are also in a position today to choose from, and compare, more than one positive-definite mass transport scheme.

The present note deals with basin-scale circulation characterized by sluggish interior flow and swift western boundary currents. The analytic simulations available to us either deal with the interior flow alone or represent a subjectively stitched-together composite of separate solutions for the interior and the boundary region. The numerical solutions, on the other hand, are obtained for flows in a closed basin and are therefore "contaminated" to some extent by interactions between the two subdomains. In light of this, we refrain in this note from expressing the proximity of analytic and numerical solutions in quantitative terms. Had we found sig-

nificant deviations between the two, we would have been forced to advise against further use of layer models in situations where outcropping plays a major role—in the context of the presently available numerical techniques, that is. Given that both transport schemes tested reproduce the analytic solutions rather closely, we feel justified in stating that accuracy problems in transport schemes allowing layer outcropping no longer appear to overshadow the customary errors associated with substituting algebraic equations for partial differential ones. This is to say that reservations about the outcrop problem in layer models should no longer be given first consideration in selecting or rejecting a model.

Acknowledgments. Support was provided by the National Science Foundation through Grants OCE-8812185 and OCE-9102560. Computations were carried out at the National Center for Atmospheric Research, sponsored by the National Science Foundation. The MPDATA module was based on code written originally by P. Smolarkiewicz. Dr. William Dewar, Florida State University, guided us in reproducing his analytic solution.

REFERENCES

Bleck, R., 1978: Finite difference equations in generalized vertical coordinates. Part I: Total energy conservation. *Contrib. Atmos. Phys.*, **51,** 360–372.

——, and D. B. Boudra, 1981: Initial testing of a numerical ocean circulation model using a hybrid (quasi-isopycnic) vertical coordinate. *J. Phys. Oceanogr.*, **11,** 755–770.

——, and ——, 1986: Wind-driven spin up in eddy-resolving ocean models formulated in isopycnic and isobaric coordinates. *J. Geophys. Res.*, **91,** 7611–7621.

Bogue, N. M., R. X. Huang, and K. Bryan, 1986: Verification experiments with an isopycnal coordinate ocean model. *J. Phys. Oceanogr.*, **16,** 985–990.

Boris, J. P., and D. L. Book, 1973: Flux-corrected transport. I.: SHASTA, A fluid transport algorithm that works. *J. Comput. Phys.*, **11,** 38–69.

Chassignet, E. P., and R. Bleck, 1993: The influence of layer outcropping on the separation of boundary currents. Part I: The wind-driven experiments. *J. Phys. Oceanogr.*, **23,** 1485–1507.

Dewar, W., 1991: Simple models of stratification. *J. Phys. Oceanogr.*, **21,** 1762–1779.

Holland, W. R., and L. B. Lin, 1975: On the generation of mesoscale eddies and their contribution to the oceanic general circulation. Part I and II. *J. Phys. Oceanogr.*, **5,** 642–669.

Huang, R. X., 1984: The thermocline and current structure in subtropical/subpolar basins. Ph.D. thesis, Massachusetts Institute of Technology, WHOI-84-42, 218 pp.

——, 1986: Numerical simulation of wind-driven circulation in a subtropical/subpolar basin. *J. Phys. Oceanogr.*, **16,** 1636–1650.

——, 1987: A three-layer model for wind-driven circulation in a subtropical-subpolar basin. Part I: Model formulation and the subcritical state. *J. Phys. Oceanogr.*, **17,** 664–678.

——, and G. Flierl, 1987: Two-layer models for the thermocline and current structure in subtropical/subpolar gyres. *J. Phys. Oceanogr.*, **17,** 872–884.

Hurlburt, H. E., and J. D. Thompson, 1980: A numerical study of loop intrusions and eddy shedding. *J. Phys. Oceanogr.*, **10,** 1611–1651.

Luther, M. E., and J. J. O'Brien, 1985: A model of the seasonal circulation in the Arabian Sea forced by observed winds. *Progress in Oceanography,* Vol. 14, Pergamon, 353–385.

Montgomery, R. B., 1937: A suggested method for representing gradient flow in isentropic surfaces. *Bull. Amer. Meteor. Soc.*, **18,** 210–212.

Rossby, C.-G., and collaborators, 1937: Isentropic analysis. *Bull. Amer. Meteor. Soc.*, **18,** 201–209.

Smolarkiewicz, P., 1984: A fully multidimensional positive definite advection transport algorithm with small implicit diffusion. *J. Comput. Phys.*, **54,** 325–362.

——, and T. L. Clark, 1986: The multidimensional positive definite advection transport algorithm: Further development and applications. *J. Comput. Phys.*, **67,** 396–438.

——, and W. W. Grabowski, 1990: The multidimensional positive definite advection transport algorithm: Nonoscillatory option. *J. Comput. Phys.*, **86,** 355–375.

Thompson, J. D., and W. J. Schmitz, 1989: A limited-area model of the Gulf Stream: Design, initial experiments, and model-data intercomparison. *J. Phys. Oceanogr.*, **19,** 791–814.

Woodberry, K., M. E. Luther, and J. J. O'Brien, 1989: The wind driven seasonal circulation in the southern tropical Indian Ocean. *J. Geophys. Res.*, **94,** 17 985–18 002.

Zalesak, S., 1979: Fully multidimensional flux-corrected transport algorithms for fluids. *J. Comput. Phys.*, **31,** 335–362.